Acc. Chem. Res. **1994**, *27*, 265−270

High Li$^+$ Conducting Ceramics

HIROMICHI AONO

Department of Industrial Chemistry, Niihama National College of Technology,
7-1 Yagumo-cho, Niihama, Ehime 792, Japan

NOBUHITO IMANAKA AND GIN-YA ADACHI*

Department of Applied Chemistry, Faculty of Engineering, Osaka University,
2-1 Yamadaoka, Suita, Osaka 565, Japan

Received January 7, 1994

Electrolytes are, in most cases, in a liquid or a molten state, and a variety of carrier ions (cations and anions) can migrate easily due to large dynamics of the matrices. In some solids, however, ions can transport very rapidly with a low energy barrier. Such solids show conductivities comparable to those of molten and aqueous electrolytes and are well-known as "solid electrolytes". One of their typical characteristics is that only one kind of carrier ion migrates because the other constituent ions are necessary to maintain the rigid structure of solid matrices.

Before the 1960s, mono- or divalent ions such as O^{2-} in "stabilized" zirconia and Ag^+ in α-AgI had been commonly known to migrate in the solid.[1-5] One of the most promising ways to obtain high ionic conducting materials is to produce vacancies for a mobile ion in the solid electrolyte. For such a purpose, tetravalent Zr^{4+} ion sites in ZrO_2 were partially substituted for di- or trivalent cations such as Ca^{2+} or Y^{3+} to form oxygen defects in the stabilized zirconia, leading to relatively easy migration of O^{2-} ions via the defects (above 900 K). On the other hand, α-AgI (the high-temperature phase) shows an extraordinarily high Ag^+ ionic conductivity though the conductivity at room temperature (β-AgI) is considerably lower. The α phase possesses a characteristic structure such that only two Ag^+ ions are statistically distributed over 42 Ag^+ vacant sites available around the I^- constituent ion per unit cell, producing so many vacancies for Ag^+ ions to pass through, and thus shows a "liquid-like" characteristic for Ag^+ ion transportation. To suppress the high-temperature (α) to the low-temperature (β) phase transition and to stabilize the highly conducting α-form even at room temperature is a natural direction to follow to get a highly conducting solid electrolyte.[6-9]

Many Ag^+ conducting materials based on AgI have been studied, and considerably higher conductivities at room temperature have been reported. However, the Ag^+ conducting electrolytes are not stable in air and easily decompose.

In the middle of the 1960s, an excellent Na^+ ion conductor,[10,11] β-alumina ($Na_2O{\cdot}11Al_2O_3$) was prepared. The alumina was at first regarded as a different phase from α-alumina (Al_2O_3) and named the β-modification. However, as shown in the chemical formula, Na^+ ions exist in the β-phase. β-Alumina is one of the typical solid electrolytes with a layered structure, and the Na^+ ions migrate between the two-dimensional conductive planes. Even for this structure, the ionic conduction is still somewhat limited due to the anisotropic conduction through the two-dimensional planes. In order to eliminate such a restriction, Goodenough and Hong[12,13] proposed a structure newly designed with a suitable tunnel size for Na^+ migration in three dimensions. This type of new material, $Na_{1+x}Zr_2Si_xP_{3-x}O_{12}$, was named as a Na^+ super ionic conductor (NASICON) in 1976. Such a well-designed polycrystalline material exhibits a high Na^+ conductivity from its characteristic structure and shows reasonable stability in air as it is based on oxides.

One important solid electrolyte application is for use as the base material for an all-solid-state rechargeable battery. A lithium battery is the most promising one owing to its high energy density and very negative electrochemical potential.[14] The energy density ($W{\cdot}h{\cdot}kg^{-1}$) of the lithium battery is about 10 times higher than that of the widely commercialized nickel−cadmium rechargeable battery. However, the lithium batteries on the market make use of some organic fluids (e.g., $LiClO_4$ dissolved in a propylene carbonate) as the electrolyte. There still remain some problems with the leakage of the organic electrolyte and of ignition in a relatively high temperature atmosphere. From these points of view, high lithium conducting

Hiromichi Aono, born in Imabar, Ehime, Japan, in 1963, received his B.E. in industrial chemistry from Ehime University. He then obtained a Ph.D. from Osaka University. He has been on the faculty in the Department of Industrial Chemistry at Niihama National College of Technology since 1986.

Nobuhito Imanaka was born in Kawanishi, Hyogo, Japan, in 1958. He earned his B.E. and M.E. in applied chemistry from Osaka University. He then obtained a Ph.D. from Osaka University. He has been on the faculty at Osaka University since 1988.

Gin-ya Adachi was born in Osaka, Japan, in 1938 and received his undergraduate degree at Kobe University. He then obtained his M.E. and Ph.D. in applied chemistry from Osaka University. In 1967 he joined the faculty at Osaka University, where he is now Professor.

---

* To whom all correspondence should be addressed.

(1) Nernst, W. *Z. Electrochem*, **1899**, *6*, 41−43.
(2) Wagner, C. *Naturwissenschaften* **1943**, *31*, 265−268.
(3) Tubandt, C. *Z. Anorg. Allg. Chem.* **1921**, *115*, 105−126.
(4) Tubandt, C.; Reinhold, H. *Z. Electrochem.* **1923**, *29*, 313−317.
(5) Strock, L. W. *Z. Phys. Chem.* **1935**, *B31*, 132−136.
(6) Reuter, B.; Hardel, K. *Naturwissenshaften* **1961**, *48*, 161.
(7) Owens, B. B.; Argue, A. G. *Science* **1967**, *157*, 308−309.
(8) Takahashi, T.; Ikeda, S.; Yamamoto, O. *J. Electrochem. Soc.* **1972**, *119*, 477−482.
(9) Tatsumisago, M.; Shinkuma, Y.; Minami, T. *Nature* **1991**, *354*, 217−218.
(10) Weber, N.; Kummer, J. T. *Proc. Annu. Power Sources Conf.* **1967**, *21*, 37−39.
(11) Whittingham, M. S.; Huggins, R. A. *J. Chem. Phys.* **1971**, *54*, 414−416.
(12) Goodenough, J. B.; Hong, H. Y.-P.; Kafalas, J. A. *Mater. Res. Bull.* **1976**, *11*, 203−220.
(13) Hong, H. Y.-P. *Mater. Res. Bull.* **1976**, *11*, 173−182.
(14) Kanehori, K.; Matsumoto, K.; Miyauchi, K.; Kudo, T. *Solid State Ionics* **1983**, *9/10*, 1445−1448.

0001-4842/94/0127-0265$04.50/0

solid electrolytes based on inorganic materials have been strongly desired and extensively investigated.

The highest Li^+ ionic conducting solids ever reported are single-crystal Li_3N and the glasses based on Li_2S.[15-20] Li_3N has a two-dimensional layered structure[15] similar to that of the above mentioned β-alumina. Li^+ can easily transport between the layers through the whole single crystal, and the conductivity of the crystal at around room temperature (1.2×10^{-3} $S{\cdot}cm^{-1}$) is close to that of 1.0 N LiCl aqueous solution (7.2×10^{-2} $S{\cdot}cm^{-1}$). For glasses based on Li_2S, a similar high conductivity (around 1×10^{-3} $S{\cdot}cm^{-1}$) was also reported at room temperature.[17-20] This high conductivity can be realized by the smaller bonding energy of Li^+—S or Li^+—I rather than that of Li^+—O, and by the larger tunnel size for Li^+ migration in vitreous materials compared with the crystalline form. However, these high Li^+ conducting electrolytes are nitride- and sulfide-based materials, and the most serious problems are deliquescence and decomposition in air.

Although oxide electrolytes are stable under humid conditions, it is commonly accepted that high Li^+ ionic conducting oxide materials cannot be obtained because of the high Li^+—O bonding energy. The highest conductivity was around 5×10^{-5} $S{\cdot}cm^{-1}$ at room temperature as for the γ_{II}-Li_3PO_4-type structure composed of MO_4 tetrahedra (M = Li, Ge, P, V, etc.) and is $^1/_{24}$ that of the Li_3N single crystal. In the γ_{II}-Li_3PO_4-type structure,[21] the tunnel size is too small for Li^+ to move because oxygen ions occupy the sites to retain a close-packed structure and considerably enforce the Li^+—O bonding. Therefore, its conductivity is 3 orders of magnitude lower than that of a 1.0 N LiCl aqueous solution. Larger tunnels are necessary to make Li^+ migration easier. The Na^+ ionic conductor such as NASICON introduced above is one of the candidate structures for a large tunnel size in three dimensions.

In this Account, we describe one of the most suitable ways for preparing a high Li^+ conducting polycrystalline material. An excellent conductivity was realized by detailed studies of both the lattice size in the Li^+ migrating bulk (intragrain) and the condition of the grain boundaries (intergrain).

Appropriate Structure for Ionic Conduction

Because of an increasing demand for high-performance batteries, a stable electrolyte with a high energy density is strongly desired. One of the candidates is a Li^+ ionic oxide conductor. However, high Li^+ conducting materials with excellent stability have not been reported so far. Taylor et al. reported that

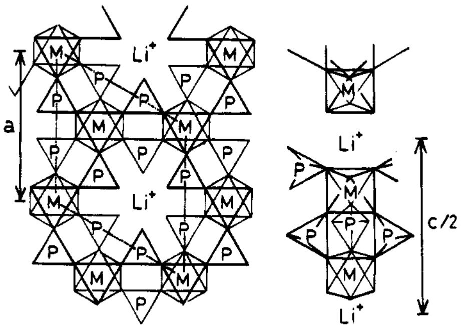

Figure 1. NASICON-type structure of $LiM_2(PO_4)_3$, M = Ge, Ti, Hf, and Zr.

Table 1. Cell Volume (Hexagonal Unit) for $LiM_2(PO_4)_3$, M = Ge, Ti, or Hf, with the M^{4+} Ionic Radius[37,38]

sample	ionic radius of M^{4+} (Å)	cell vol (Å^3)
$LiGe_2(PO_4)_3$	0.540	1218
$LiTi_2(PO_4)_3$	0.605	1309
$LiHf_2(PO_4)_3$	0.710	1486

$LiM_2(PO_4)_3$, M^{IV} = Ge,[22,23] Ti,[24-32] Hf,[33] and Zr,[34,35] forms a three-dimensional isotropic NASICON-type structure as shown in Figure 1. Two types of polyhedra, MO_6 octahedra and PO_4 tetrahedra, are linked by their corners to form the $[M_2(PO_4)_3]^-$ rigid skeleton, and Li^+ ion migrates through the tunnel three-dimensionally in the structure.[36] The tunnel size for the structure is easily adjusted by changing the substituting tetravalent cation in $LiM^{IV}{}_2(PO_4)_3$. The cell volume (hexagonal unit) of $LiM_2(PO_4)_3$ (M = Ge, Ti, and Hf)[37] and the M^{4+} ionic radius[38] are summarized in Table 1. The NASICON-type structure suitable for ionic conduction was obtained for these three systems, and the cell volume is simply dependent on the ionic size of the M^{4+} ions.

Suitable Skeleton Size for Li^+ Ion Migration

The Li^+ intragrain migration is directly affected by the change of the lattice size caused by the ion substitution. Figure 2 shows the relationship between

---

(15) Alpen, U. v.; Rabenau, A.; Talat, G. H. *Appl. Phys. Lett.* **1977**, *30*, 621–623.

(16) Boukamp, B. A.; Huggins, R. A. *Mater. Res. Bull.* **1978**, *13*, 23–32.

(17) Mercier, R.; Malugani, J. P.; Fahys, B.; Saida, A. *Solid State Ionics* **1981**, *5*, 663–666.

(18) Wada, H.; Menetrier, M.; Levasseur, A.; Hagenmuller, P. *Mater. Res. Bull.* **1983**, *18*, 189–193.

(19) Kennedy, J. H.; Sahami, S.; Shea, S. W.; Zhang, Z. *Solid State Ionics* **1985**, *18/19*, 368–371.

(20) Kondo, S.; Takada, K.; Yamamoto, Y. *Solid State Ionics* **1992**, *53–56*, 1183–1186.

(21) Rodger, A. R.; Kuwano, J.; West, A. R. *Solid State Ionics* **1985**, *15*, 185–198.

(22) Li, S.-c.; Cai, J.-y.; X.; Lin, Z.-x. *Solid State Ionics* **1988**, *28–30*, 1265–1270.

(23) Aono, H.; Sugimoto, E.; Sadaoka, Y.; Imanaka, N.; Adachi, G. *Bull. Chem. Soc. Jpn.* **1992**, *65*, 2200–2204.

(24) Shi-chun, L.; Zu-Xiang, L. *Solid State Ionics* **1983**, *9/10*, 835–838.

(25) Zu-xiang, L.; Hui-jun, Y.; Shi-chun, L.; Shun-Bao, T. *Solid State Ionics* **1986**, *18/19*, 549–552.

(26) Zu-xiang, L.; Hui-jun, Y.; Shi-chun, L.; Shun-Bao, T. *Solid State Ionics* **1988**, *31*, 91–94.

(27) Subramanian, M. A.; Subramanian, R.; Crearfield, A. *Solid State Ionics* **1986**, *18/19*, 562–569.

(28) Hamdoune, S.; Tranqui, D. *Solid State Ionics* **1986**, *18/19*, 587–591.

(29) Tran qui, D.; Hamdoune, S.; Soubeyroux, J. L.; Prince, E. *J. Solid State Chem.* **1988**, *72*, 309–315.

(30) Aono, H.; Sugimoto, E.; Sadaoka, Y.; Imanaka, N.; Adachi, G. *J. Electrochem. Soc.* **1989**, *136*, 590–591.

(31) Aono, H.; Sugimoto, E.; Sadaoka, Y.; Imanaka, N.; Adachi, G. *J. Electrochem. Soc.* **1990**, *137*, 1023–1027.

(32) Aono, H.; Sugimoto, E.; Sadaoka, Y.; Imanaka, N.; Adachi, G. *Chem. Lett.* **1990**, 1825–1828.

(33) Aono, H.; Sugimoto, E.; Sadaoka, Y.; Imanaka, N.; Adachi, G. *Solid State Ionics* **1993**, *62*, 309–316.

(34) Taylor, B. E.; English, A. D.; Berzins, T. *Mater. Res. Bull.* **1977**, *12*, 171–182.

(35) Petit, D.; Colomban, Ph.; Collin, G.; Boilot, J. P. *Mater. Res. Bull.* **1986**, *21*, 365–371.

(36) Hagman, L.; Kierkegaard, P. *Acta Chem. Scand.* **1968**, *22*, 1822–1832.

(37) Aono, H.; Sugimoto, E.; Sadaoka, Y.; Imanaka, N.; Adachi, G. *J. Electrochem. Soc.* **1993**, *140*, 1827–1833.

(38) Shannon, R. D. *Acta Crystallogr.* **1976**, *A32*, 751–767.

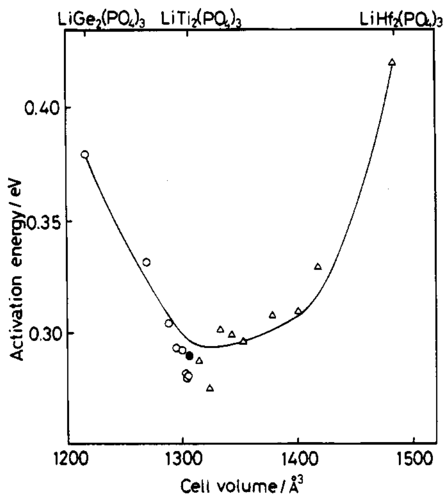

Figure 2. Relationship between the activation energy for Li$^+$ intragrain migration and the cell volume (hexagonal unit) for $LiM_xTi_{2-x}(PO_4)_3$ bulk [x = 0 (●), M = Ge (○), Hf (△)].

the activation energy for Li$^+$ ion intragrain migration and the cell volume for $LiM_xTi_{2-x}(PO_4)_3$.[37] The cell volume changes with the M^{4+} (M = Ge and Hf) ions substituted. The minimum activation energy (ca. 0.30 eV) is obtained for the samples with the cell volume around 1310 Å^3. The activation energy appreciably increases when the cell volume is smaller or larger than that of $LiTi_2(PO_4)_3$. This clearly indicates that the $LiTi_2(PO_4)_3$ structure has the most suitable lattice size for Li$^+$ migration. A smaller tunnel size makes the carrier Li$^+$ migration more difficult, while a larger size leads Li$^+$ to approach the oxygens of the polyhedra because of a high Li$^+$—O bonding energy. As a result of the stronger Li$^+$—O attraction, higher activation energy is needed to overcome the Li$^+$—O bonding and transport in the bulk. A similar phenomenon is observed for β-alumina, composed of the two-dimensional layer strucrture as described above. The activation energy of ion migration for Li$^+$ in β-alumina (Li$^+$ ionic radius: 0.76 Å)[38] is higher than that for Na$^+$ in β-alumina (Na$^+$: 1.02 Å[38]).[39,40]

Conductivities

The conductivity of $LiTi_2(PO_4)_3$ is rather low. However, it increases above 10^{-4} S·cm^{-1} at room temperature when one of the constituent cations, Ti^{4+}, is partially replaced by trivalent cations[24-32] and not tetravalent cations. The cell volume resulting from such a partial substitution ranges from 1300 to 1350 Å^3, which is within the region of the smallest activation energy (see Figure 2). The variability of ionic radius among the trivalent cations hardly influences the conductivity.

Figure 3 presents the conductivity at 298 K for the three-dimensionally isotropic ionic conductors of $LiGe_2(PO_4)_3$-based, $LiTi_2(PO_4)_3$-based, and $LiHf_2(PO_4)_3$-based systems.[23,31,33] The porosity decreases similarly for these three systems, as shown in Figure 3. The M^{3+} ion substitution greatly enhanced the conductivity to higher than 10^{-4} S·cm^{-1} for all the systems with decreased porosity, whereas a high-density sample

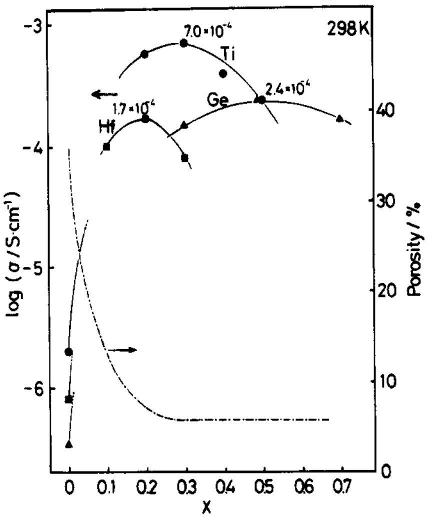

Figure 3. The Li$^+$ conductivity at 298 K and the porosity for the NASICON-type solids: $Li_{1+x}Al_xGe_{2-x}(PO_4)_3$ system (▲), $Li_{1+x}Al_xTi_{2-x}(PO)_4)_3$ system (●), $Li_{1+x}Fe_xHf_{2-x}(PO_4)_3$ system (■), porosity —·—.

cannot be obtained without the M^{3+} substitution. The Li$^+$ conductivities for the NASICON-type materials are the highest for the Li$^+$ conducting oxide-based electrolytes. Especially, the conductivity for the Ti-based system (7.0 x 10^{-4} S·cm^{-1}) is comparable to that of the highest Li$^+$ conducting materials, such as Li_3N single crystal and Li_2S-based glasses. The conductivity enhancement due to the M^{3+} ion substitution is not related to the ionic radius of the substituting M^{3+} ions but closely related to the sinterability.

Reason for the Conductivity Enhancement

The resistivity of the polycrystalline electrolyte is obtained by summing the bulk (ϱ_b) and the grain boundary (ϱ_{gb}) resistivities, which can be determined individually by a complex impedance analysis (Cole–Cole plot). By this method, the total resistivity can be divided easily into ϱ_b and ϱ_{gb} components. The impedance approaches the bulk resistivity (ϱ_b) in the higher frequency region and thus the total resistivity ($\varrho_b + \varrho_{gb}$) in the lower frequency region, because the capacitance of the grain boundary is appreciably larger than that of the bulk component. The total conductivity (σ) can be obtained from the reciprocal of the total resistivity [$1/(\varrho_b + \varrho_{gb})$].

Figure 4 shows the relation between the conductivity (σ) and temperature (T) for the bulk (intragrain), the grain boundary, and the total conductivity of $LiTi_2(PO_4)_3$ and $Li_{1.3}Al_{0.3}Ti_{1.7}(PO_4)_3$.[41,42] A straight line was obtained in the $\log(\sigma T)-1/T$ relation of both the bulk and the grain boundary components. The activation energy for Li$^+$ migration can be calculated from the Arrhenius equation,

$$\sigma T = \sigma_0 \exp(E/kT) \qquad (1)$$

where T, σ_0, E, and k denote the absolute temperature, preexponential factor, activation energy for ionic migration, and Boltzmann's constant, respectively. The total conductivity at around room temperature was mainly controlled by that of the grain boundary

---

(39) Whittingham, M. S.; Huggins, R. A. *NBS Spec. Publ.* (*Solid State Chem.*) **1972**, *364*, 139–154.

(40) Briant, J. L.; Farrington, G. C. *J. Electrochem. Soc.* **1981**, *128*, 1830–1834.

(41) Bauerle, J. E. *J. Phys. Chem. Solids* **1969**, *30*, 2657–2670.

(42) Bruce, P. G.; West, A. R. *J. Electrochem. Soc.* **1983**, *130*, 662–669.

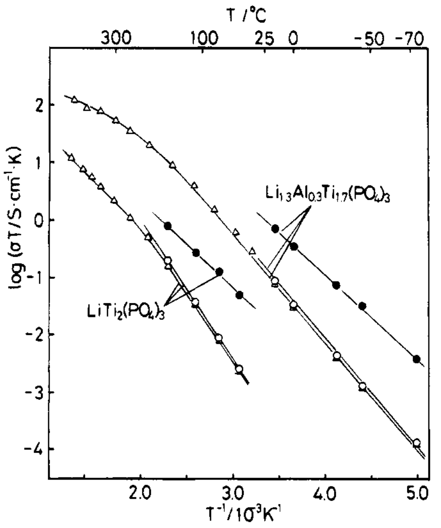

Figure 4. The log(σT)$-1/T$ relation of the bulk, the grain boundary, and the total for the samples of LiTi$_2$(PO$_4$)$_3$ and Li$_{1.3}$Al$_{0.3}$Ti$_{1.7}$(PO$_4$)$_3$: bulk (●), grain boundary (○), total (△).

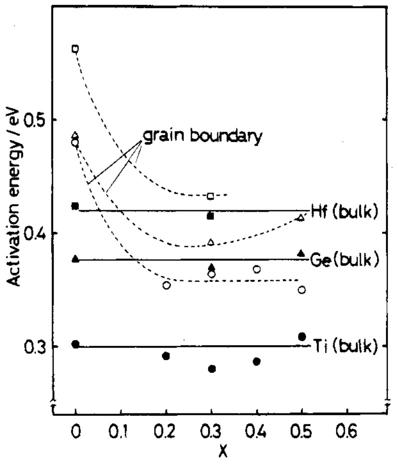

Figure 5. The activation energies of the bulk component and the grain boundary for the NASICON-type solids. Li$_{1+x}$Al$_x$Ge$_{2-x}$(PO$_4$)$_3$ system: bulk (▲), grain boundary (△). Li$_{1+x}$Al$_x$Ti$_{2-x}$(PO$_4$)$_3$ system: bulk (●), grain boundary (○). Li$_{1+x}$Fe$_x$Hf$_{2-x}$(PO$_4$)$_3$ system: bulk (■), grain boundary (□).

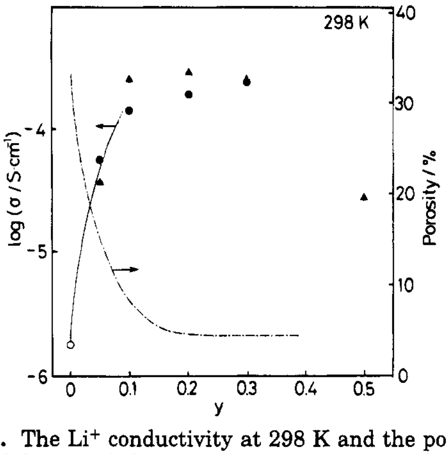

Figure 6. The Li$^+$ conductivity at 298 K and the porosity for the LiTi$_2$(PO$_4$)$_3$ + y(lithium salt) systems: LiTi$_2$(PO$_4$)$_3$ + yLi$_3$PO$_4$ system (●), LiTi$_2$(PO$_4$)$_3$ + yLi$_3$BO$_3$ system (▲), porosity —·—.

component. On the contrary, at higher temperatures (above ca. 250 °C), the total conductivity is governed by that of the bulk component. A gentle curvature of the total conductivity at around 250 °C is mainly ascribed to the difference in the slope of the log(σT)$-$1/T relation between the bulk and the grain boundary components.

The activation energies for Li$^+$ conduction of the bulk and the grain boundaries are calculated from eq 1 and depicted in Figure 5. The activation energies for the bulk component are constant at 0.38, 0.30, and 0.42 eV for the Ge, Ti, and Hf systems irrespective of the replaced trivalent ion amount. Since an M^{3+} ion substitutes an M^{4+} site, the Li$^+$ amount increased by the replacement is exactly the same as the amount replaced by the M^{3+} ion for the charge compensation. The increase of the lithium amount by the M^{3+} substitution did not influence the Li$^+$ mobility of the bulk. On the other hand, the activation energy at the grain boundary decreased for all three systems with the M^{3+} amount. The tendency of the decrease in the activation energy is quite similar to that of the porosity reduction (Figure 3). The conductivity enhancement by the M^{3+} ion substitution in LiM$_2$(PO$_4$)$_3$ (M^{4+} = Ge^{4+}, Ti^{4+}, and Hf^{4+}) is mainly attributed to the decrease in the activation energy at the grain boundary by the high densification as already shown in Figure 3. The control of the grain boundary condition is a key factor in obtaining a suitable polycrystalline room temperature solid electrolyte, because the electrical properties for the NASICON-type polycrystalline materials are mainly controlled by the grain boundary component at around room temperature.

One of the promising methods to eliminate grain boundaries is to vitrify the polycrystal. The vitreous form is essentially free from a low conductive grain boundary. In fact, the advantage of a vitrification has been reported for polycrystalline electrolytes such as Li$^+$ mobile LiNbO$_3$ and Ag$^+$ conductive AgI$-$Ag$_2$MoO$_4$ systems.[43-45] In these samples, the conductivity increases due mainly to the enlargement of the tunnel size for the ion migration and to the elimination of the grain boundary. The glassy LiTi$_2$(PO$_4$)$_3$ and Li$_{1.3}$Al$_{0.3}$Ti$_{1.7}$(PO$_4$)$_3$ samples were also prepared by a rapid quenching method[46] or an explosion method.[47] However, their conductivities are appreciably lower than those of the polycrystalline conductors. Although grain boundaries are not present in the vitreous solid, the bulk does not hold a suitable tunnel size for Li$^+$ migration at all, since a rigid [Ti$_2$(PO$_4$)$_3$]$^-$ skeleton, which is needed to conduct Li$^+$ smoothly, was almost destroyed by the vitrification. The vitrifying treatment is not an appropriate method to obtain high ionic conduction for such a three-dimensional skeleton solid.

Addition of the Lithium Salts

The addition of lithium salts such as Li$_3$PO$_4$ or Li$_3$BO$_3$ into LiM$_2$(PO$_4$)$_3$, M = Ge, Ti, or Hf,[37,48,49] is also quite effective to elevate the conductivity. Figure 6 depicts the conductivity for the LiTi$_2$(PO$_4$)$_3$ + y(lithium

---

(43) Glass, A. M.; Nassau, K.; Negran, T. J. *J. Appl. Phys.* **1978**, *49*, 4808–4811.

(44) Minami, T.; Nambu, H.; Tanaka, M. *J. Am. Ceram. Soc.* **1977**, *60*, 283–284.

(45) Minami, T.; Nambu, H.; Tanaka, M. *J. Am. Ceram. Soc.* **1977**, *60*, 467–469.

(46) Machida, N.; Fujii, K.; Minami, T. *Chem. Lett.* **1991**, 367–370.

(47) Imanaka, N.; Shimizu, T.; Adachi, G. *Solid State Ionics* **1993**, *62*, 167–171.

(48) Aono, H.; Sugimoto, E.; Sadaoka, Y.; Imanaka, N.; Adachi, G. *Solid State Ionics* **1991**, *47*, 257–264.

(49) Aono, H.; Sugimoto, E.; Sadaoka, Y.; Imanaka, N.; Adachi, G. *Chem. Lett.* **1990**, 331–334.

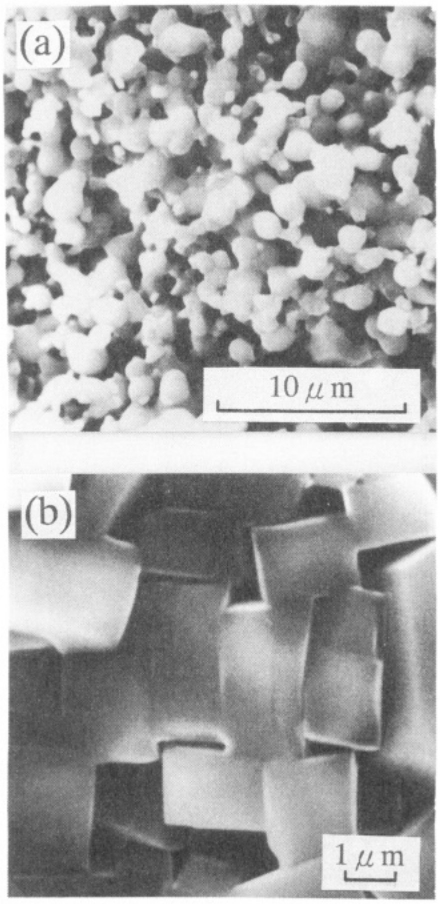

Figure 7. The surface microstructure of the sintered pellets: (a) $LiTi_2(PO_4)_3$ (sintered at 1433 K); (b) $LiTi_2(PO_4)_3$ + $0.2Li_3PO_4$ (sintered at 1173 K).

salt) system, where the addition of lithium salt greatly enhances the conductivity. The maximum conductivity (3×10^{-4} S·cm^{-1}) is almost equal to that of the M^{3+}-substituted systems. The lithium salt does not make a solid solution with $LiTi_2(PO_4)_3$ and only works as a binder in obtaining high-density ceramics and conductivity enhancement. The activation energy of Li^+ migration at the grain boundary also decreases by the addition of the lithium salt, but that at the bulk component was constant. These results are similar to the case for the M^{3+}-substituted $Li_{1+x}M^{III}_xM^{IV}_{2-x}(PO_4)_3$ systems.[30–32]

Figure 7 shows the surface microstructure of the sintered pellets for $LiTi_2(PO_4)_3$ without lithium salt (a) and $LiTi_2(PO_4)_3$ + $0.2Li_3PO_4$ (b). $LiTi_2(PO_4)_3$ is porous, and a high-density sample cannot be obtained. For $LiTi_2(PO_4)_3$ with Li_3PO_4 salt, the crystalline grains have obviously grown in close contact with one other, indicating that high-density ceramics are easily formed. By the close contact, most of the directions of neighboring grains match each other, thus resulting in high sinterability. As a result of this uniformity, the tunnel for Li^+ migration comes to be more probably connected. The additional lithium salt contributes to obtaining a high-density solid with a highly conductive grain boundary layer.

For the M^{3+}-substituted samples, the high densification by sintering was accomplished without any binders. The highly conductive grain boundaries might be formed by a solid diffusion process. Although the high densification occurs with the aid of the binders for the samples with lithium salts, and occurs by the solid diffusion process for the M^{3+}-substituted samples, both ceramics have a quite similar ion-conducting layer at the grain boundary.

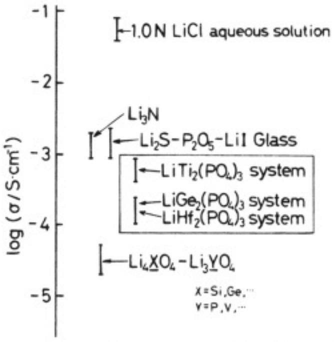

Figure 8. The ionic conductivity at 298 K for the various Li^+ conducting solids and a 1.0 N LiCl aqueous solution.

Applications

Figure 8 presents the Li^+ conductivities at 298 K for the isotropic three-dimensional materials and representative high Li^+ conducting electrolytes. It is commonly accepted that any Li^+ conducting oxide based materials cannot be obtained because of the strong Li^+–O bonding. The conductivities for the NASICON-type solid phosphates surrounded by a solid square show superior conductivity. The maximum conductivity in such Li^+ conductors is 7.0×10^{-4} S·cm^{-1} for $Li_{1.3}Al_{0.3}Ti_{1.7}(PO_4)_3$. However, the Ti^{4+} ion in the conductor is easily reduced by Li metal when used as an electrode.[50] This Ti-based material is rather suitable as a cathode for a lithium battery, since lithium insertion is readily realized in lithium titanium(III/IV) phosphate, $Li_{1+x}Ti_2(PO_4)_3$ ($0 \le x \le 2.0$) series.[51–55] Li_3N single crystal or Li_2S-based glasses are also high lithium conductive materials. However, there still remains a severe problem in lithium battery applications because of their instabilities in the atmosphere and strong hygroscopic properties. As an electrolyte for the lithium battery, $LiGe_2(PO_4)_3$-based or $LiHf_2(PO_4)_3$-based systems are more promising materials among the Li^+ conductors presented in Figure 8 for their high lithium ionic conductivity and superior stability toward the Li metal electrode.

Conclusion

The three-dimensional network structure presented here seems to be an optimum one for Li^+ migration in the oxide electrolytes. The control of the grain boundaries is the most important factor in obtaining a superior Li^+ conducting polycrystalline ceramic. The NASICON-type $LiM_2(PO_4)_3$ (M = Ge, Ti, or Hf) materials show not only low conductivity but also poor sinterability. However, both problems are greatly improved by the M^{4+} site substitution for M^{3+} ion or by the addition of lithium compounds to the phosphate. The ion substitution in $LiM_2(PO_4)_3$ or the

---

(50) Aono, H.; Sugimoto, E.; Sadaoka, Y.; Imanaka, N.; Adachi, G. *Chem. Lett.* **1991**, 1567–1570.

(51) Varadaraju, U. V.; Thomas, K. A.; Sivasankar, B.; Rao, G. V. S. *J. Chem. Soc., Chem. Commun.* **1987**, 814–815.

(52) Delmas, C.; Nadiri, A.; Soubeyroux, J. L. *Solid State Ionics* **1988**, *28–30*, 419–423.

(53) Wang, S.; Hwu, S.-J. *J. Solid State Chem.* **1991**, *90*, 377–381.

(54) Wang, S.; Hwu, S.-J. *Chem. Mater.* **1992**, *4*, 589–595.

(55) Wang, B.; Greenblatt, M.; Wang, S.; Hwu, S.-J. *Chem. Mater.* **1993**, *5*, 23–26.

addition of the lithium compound to the phosphate leads to the formation of a high conductive grain boundary layer and a high-density sintered pellet resulting in the enhancement of the total ionic conductivity. Among the various NASICON-type materials, the $LiTi_2(PO_4)_3$-based one has the most suitable lattice size and shows the highest ionic conductivity with a minimum activation energy for Li^+ migration in the bulk. The phosphates with Ge or Hf are promising materials in the NASICON-type $LiM_2(PO_4)_3$ series from a practical viewpoint in the application of all solid-state rechargeable batteries.

The present work was partially supported by Grants-in-Aid for Scientific Research No. 02555163 (G.A.), No. 02750579 (H.A.), No. 03205082 (G.A.), No. 04205091 (G.A.), and No. 04855146 (H.A.) from the Ministry of Education, Science and Culture.